DOI: 10.61782/fa.2025.0503

FORUM ACUSTICUM
EURONOISE 2025

INVESTIGATION OF MEMORY EFFICIENT CONVOLUTION TRUNCATION METHODS FOR THE 2D TIME DOMAIN BOUNDARY ELEMENT METHOD

Doğuhan Kılıçarslan [1,2*] **Dionysios Panagiotopoulos**[1,2] **Elke Deckers**[1,2]

[1] Department of Mechanical Engineering, KU Leuven, Belgium
[2] Flanders Make @KU Leuven, Belgium

ABSTRACT

Transient numerical simulations are typically used to auralize sound sources and in particular for problems including moving sources. The time domain boundary element method (TD-BEM) is a particularly attractive alternative as it is especially suitable for exterior/unbounded domains. Nevertheless, as TD-BEM uses the fundamental solution together with a convolution integral to obtain the solution; a new system matrix is assembled for each time step and used together with all previously assembled system matrices to calculate the response for the current time step. Thus, the memory required to store the system matrices grows with time, possibly resulting in an excessive requirement. To alleviate this issue, several techniques resort to either efficient truncations of the convolution calculation at later time instances or interpolation strategies of the fundamental solution in time. In this work, the truncation method for 2D TD-BEM is extended using higher order Taylor series expansion, focusing on a better trade-off between memory reduction and numerical error. In particular, the effect of changing the expansion order and the representative distance on the error is examined for interior and exterior examples. Results lead to the conclusion that larger storage reduction is obtained by including higher order terms while the error remains acceptable.

*Corresponding author: doguhan-nuri.kilicarslan@kuleuven.be.

Keywords: *time domain,boundary element method, time truncation, memory reduction*

1. INTRODUCTION

The boundary element method (BEM) is used quite extensively for numerical acoustical analysis in the frequency domain [1], while its application for time domain simulations is a less studied topic [2]. Even for applications where the time domain should have the advantage, frequency domain BEM is used such as is the case for pass-by-noise analysis [3] or auralization using head related transfer functions [4]. Instead of directly using time domain solutions, those simulations rely on the construction of time domain response by utilizing convolution of the frequency response functions.

One of the main issues of employing the time domain BEM (TD-BEM) is that the stability of the solution is problem dependent [5]; however, it can be mended with different formulations [6] or different convolution calculations [7]. Additionally, one of the main drawbacks of the TD-BEM is that the formulation requires the explicit calculation of convolution, since the fundamental solution is non-affinely dependent on time [8]. This convolution calculation increases the computational effort, requiring the construction of new system matrices for each time step and performing matrix-vector multiplications for all previous time steps to capture their effects. This results not only in increasing the memory requirements for the storage of the system matrices, but also an unfavorably scaling multiplication costs. This holds especially for the two dimensional case where the fundamental solution is a step

function with a slow decay in time, resulting in fully populated system matrices after certain time [9].

Several mitigation strategies have been proposed to alleviate the storage difficulty. Starting with the works of Demirel and Wang [9] where the convolution calculation is fully stopped after a predetermined cutoff time separation (t_L), which can be calculated based on the ratio of the remaining area under the fundamental solution to the already calculated area (δ). The ratio δ acts as an error estimator as well as a storage/cost reduction metric. Even though truncation seems to work for exterior problems with no reflections, it creates significant error for interior problems where reflections are present. Instead, for interior domains, the problem can be tackled with partial truncation by Mansur and Delima-Silva [10] that replaces all the distances in the boundary integral calculation by a constant average distance (r_{avg}) by assuming time separation is much larger compared to the physical domain. Then, instead of truncating the convolution after t_L; a single system matrix constructed with r_{avg} is stored and employed after multiplying it with a function that depends only on time during the convolution calculations.

Even though high storage cost reductions can be achieved with partial or total truncation, errors which do not have robust estimators might increase rapidly, while only limited storage cost is gained. Hence, interpolating polynomials, such as Lagrange or radial basis functions [11], have been proposed for the separation of time convolution and boundary integration. Such techniques succeed in minimizing calculation efforts by only calculating the system matrices at predefined positions in time, and interpolating for the intermediate time steps. Nevertheless, interpolation methods generally require multiple additional system matrices to be stored as compared to the truncation methods. On the other hand, the error obtained with interpolation is much smaller, such that larger t_L can be chosen, therefore reducing the total system matrices to be constructed [12].

In this work, the truncation approach is extended by considering a series expansion strategy of the analytically integrated kernel produced by linear and constant time interpolation for pressure and flux, respectively. The kernel is expanded around a representative distance with Taylor series such that time convolution and the domain integral can be separated. The resulting formulation produces lower errors with increasing approximation order, enabling the choice of a larger t_L. The resulting acceleration method is validated on two academic examples with known analytical solutions and on a complex geometry.

2. TD-BEM FPRMULATION

TD-BEM for the 2-dimensional scalar wave equation is given by Mansur [13] and can be written as:

$$\begin{aligned}(\mathbf{H}_{nn}+\mathbf{C})\,\mathbf{p}_n+\mathbf{G}_{nn}\mathbf{q}_n=\\ \mathbf{f}_n+\sum_{m=1}^{n-1}\left(\mathbf{H}_{nm}\mathbf{p}_m+\mathbf{G}_{nm}\mathbf{q}_m\right)\end{aligned} \tag{1}$$

where $\mathbf{H}_{nm}$ and $\mathbf{G}_{nm}$ are system matrices calculated for time steps n and m representing the emitter and receiver times; $\mathbf{p}_n$, $\mathbf{q}_n$, and $\mathbf{f}_n$ are the vectors relating to pressure, flux, [1] and source values for discrete boundary points for discrete time step n, respectively. $\mathbf{C}$ is the free term coefficient calculated as is done in the frequency domain formulation [13]. Moreover $\mathbf{H}_{nm}$ and $\mathbf{G}_{nm}$ are defined as the discrete form of the boundary integral equations

$$H(\boldsymbol{x},t)=\int_\Gamma \tfrac{\partial(\boldsymbol{x}-\boldsymbol{\xi})}{\partial n}\int_0^t\left(q^*p+p^*\tfrac{1}{c}\tfrac{\partial p}{\partial\tau}\right)d\tau\,d\Gamma, \tag{2a}$$

$$G(\boldsymbol{x},t)=\int_\Gamma\int_0^t p^*q\,d\tau\,d\Gamma, \tag{2b}$$

where $\boldsymbol{x}$ is a point on the boundary [2] while $\boldsymbol{\xi}$ is the secondary position vector on the boundary for integration. Furthermore, the pressure and flux fundamental solutions p^* and q^* are defined as the impulse response emitted at time τ, and measured at a time t with a distance $r=|\boldsymbol{x}-\boldsymbol{\xi}|$ away from the source and given mathematically as

$$p^*=\frac{2c}{\sqrt{c^2(t-\tau)^2-r^2}}\,\hat{H}\left(c(t-\tau)-r\right), \tag{3a}$$

$$q^*=\frac{2c\left(c(t-\tau)-r\right)}{\sqrt{c^2(t-\tau)^2-r^2}}\,\hat{H}\left(c(t-\tau)-r\right), \tag{3b}$$

where c is the speed of sound and $\hat{H}$ is the Heaviside step function such that information travels at speed c and the causality of the problem is respected. The time integral of Eqn. (2) can be analytically calculated utilizing linear interpolation for pressure and constant interpolation for flux (for more details see [8]), with the resulting intermediate kernels H^*_{nm} and G^*_{nm} that can be used in boundary integration.

[1] Flux here is used vaguely referring to the gradient of pressure, if the velocity potential formulation for acoustics were to be used it would refer to particle velocity.

[2] It can refer to a point in the domain to calculate the domain response from boundary values for post-processing.

Note that all the descriptions are made on the assumption that time steps are equidistant such that H^*_{nm} and G^*_{nm} only depend on the time separation between time steps $(n-m)\Delta t$. Otherwise, the formulation scales with $O(N_T^2)$ instead of $O(N_T)$, N_T being the total time steps.

2.1 Singularities and wavefront

Kernels p^* and q^* demonstrate two different singularities; one is a geometric singularity that occurs when $r \to 0$, and the other one is the wavefront singularity that occurs when $c(t-\tau) \to r$. However, H^*_{nm} and G^*_{nm} are not affected by these singularities due to subtractive cancelations [14].
The only remaining singularity arises for H^*_{nm} when $n-m=0$ (i.e. observation time step and emission time step are the same). Nonetheless, the calculation of the singular integral is not necessary if constant or linear spatial elements are used, because H^*_{nm} and the respective shape function gradient $\frac{\partial(\boldsymbol{x}-\boldsymbol{\xi})}{\partial n}$ in Eqn. (2a) are orthogonal. Even though the wavefront singularity is eliminated, it still disturbs the smoothness of the intermediate kernels as $n-m$ gets closer to zero. Thus, smooth approximations to H^*_{nm} and G^*_{nm}, such as Taylor series, might become inadequate; which is a limiting factor in the current study.

2.2 Total truncation

As can be seen from Eqn. (1), in order to calculate a new convolution for each time step n, all past responses need to be multiplied with the corresponding past system matrix and summed. Resulting calculation and storage costs scale quadratically and linearly with time, respectively. The initial remedy to this shortcoming is to disregard the terms in the convolution summation of Eqn. (1), that are separated by more than $t_L = N_L\Delta t$ [9]. This cutoff time is based on the δ parameter, which is defined as

$$\delta = \int_0^{t_F - t_L} p^* d\tau \Big/ \int_0^{t_F - r_{avg}} p^* d\tau \ , \tag{4}$$

where $t_F = N_T\Delta t$ is the final time of the simulation and r_{avg} is the average distance of the domain. Hence, parameter δ corresponds to the ratio of the lost information if the integral of p^* is truncated after t_L at a distance $r = r_{avg}$. Thus, δ is not an actual error predictor of the solution but a rather crude approximation of error for H^*_{nm} and G^*_{nm}. Finally, the equation of motion (1) can be written for $n > N_L$ as

$$\begin{aligned}&(\mathbf{H}_{nn} + \mathbf{C})\,\mathbf{p}_n + \mathbf{G}_{nn}\mathbf{q}_n = \\ &\mathbf{f}_n + \sum_{m=n-N_L}^{n-1} \left(\mathbf{H}_{nm}\mathbf{p}_m + \mathbf{G}_{nm}\mathbf{q}_m\right).\end{aligned} \tag{5}$$

The resulting solution requires N_L/N_T relative storage and computational costs compared to full solution while introducing an approximation error.

2.3 Partial truncation

The next development is to increase the reduction by decreasing the resulting error by the inclusion of single set of matrix calculation. Since kernels p^* and q^* are dominated by time contributions for $t_L \gg r/c$, contributions related to r can be ignored. This is achieved by using $r = r_{avg}$ to avoid additional singularities, such that for $n > N_L$ the term

$$\sum_{m=1}^{n-N_L-1} \left(\mathbf{H}^{(1)} h^{(1)}_{nm}\mathbf{p}_m + \mathbf{G}^{(1)} g^{(1)}_{nm}\mathbf{q}_m\right) \tag{6}$$

is added to to Eqn. (5) where $\mathbf{H}^{(1)}$ and $\mathbf{G}^{(1)}$ are matrices calculated by the boundary integral with the kernel "1"; moreover, $h^{(1)}_{nm}$ and $g^{(1)}_{nm}$ are functions of time defined by the substitution of $r = r_{avg}$ in Eqns. (3), respectively. Partial truncation strategy requires an additional set of system matrices compared to total truncation strategy while reducing the error significantly. Such that smaller error enables the selection of larger t_L values, which lowers the storage and computational costs compared to the total truncation strategy.

3. SERIES EXPANSION TD-BEM

Even though, partial truncation offers significant advantages, its applicability is limited due to the initial assumption of $t_L \gg r/c$. In contrast, attempting to remedy the storage and cost problem by a spatial reduction can offer higher order expansion terms. Assuming that the kernels p^* and q^* are smooth functions of r, they can be expanded around a representative distance $r = r_{rep}$ with a Taylor series expansion. As noted in Sec. 2.2, although this assumption starts to fail as time separation becomes smaller, it allows greater generalization compared to the assumptions made in the partial truncation approach. Specifically, by explicitly expanding p^* and q^* around $r = r_{rep}$ it can

be written

$$p^* = \frac{2c}{\sqrt{c^2(t-\tau)^2 - r_{rep}^2}} + \frac{2cr_{rep}(r-r_{rep})}{\left(c^2(t-\tau)^2 - r_{rep}^2\right)^{3/2}} + \dots, \quad (7a)$$

$$q^* = \frac{2c(c(t-\tau)-r_{rep})}{\sqrt{c^2(t-\tau)^2 - r_{rep}^2}} - \frac{2c^2(t-\tau)(r-r_{rep})}{(c(t-\tau)+r_{rep})\sqrt{c^2(t-\tau)^2 - r_{rep}^2}} + \dots. \quad (7b)$$

In the above expressions, the first term is treated identically as in the partial truncation approach. However, higher order terms are quite lengthy and require significant effort while integrating analytically in time. To simplify the implementation, H^*_{nm} and G^*_{nm} can be expanded with Taylor series instead of p and q; the resulting expressions for $t > r_{max}/c$ are given as

$$H^*_{nm} = h_{n,m+1} - 2h_{n,m} + h_{n,m-1}, \quad (8a)$$

$$G^*_{nm} = g_{n,m} - g_{n,m-1}, \quad (8b)$$

where $h_{n,m}$ and $g_{n,m}$ are used to replace repetitive expressions and are defined as

$$h_{n,m} = \sqrt{\frac{c^2\Delta t^2 (n-m)^2}{r^2} - 1}, \quad (9a)$$

$$g_{n,m} = \ln\left(\frac{c\Delta t\,(n-m)}{r} - h_{n,m}\right). \quad (9b)$$

Furthermore, expanding H^*_{nm} and G^*_{nm} around $r = r_{rep}$ results in the following higher order system matrices

$$\mathbf{H}^{(k)} = \int_\Gamma \frac{\partial r}{\partial n}\,(r - r_{rep})^{k-1}\,d\Gamma, \quad (10a)$$

$$\mathbf{G}^{(k)} = \int_\Gamma (r - r_{rep})^{k-1}\,d\Gamma. \quad (10b)$$

The temporal functions $h^{(k)}_{nm}$ and $g^{(k)}_{nm}$ are defined by the Taylor series terms of H^*_{nm} and G^*_{nm} defined by Eqn. (8) calculated considering $r = r_{rep}$, which are straightforward to calculate and for the sake of brevity are omitted in this work. Finally, in order to express the equation of motion, the expression

$$\sum_{m=1}^{n-N_L-1}\left(\sum_{k=1}^{N_o}\mathbf{H}^{(k)}h^{(k)}_{nm}\mathbf{p}_m + \mathbf{G}^{(k)}g^{(k)}_{nm}\mathbf{q}_m\right) \quad (11)$$

needs to be added to the Eqn. (5). Since the reduced matrices now include distances with different orders, geometrical information is retained to a certain extent, compared to partial truncation.

4. RESULTS

4.1 Interior response for a rectangular geometry with impulsive boundary excitation

The first example is the interior rectangular geometry shown in Fig. 1 with side lengths $L_x = 2\ m$, $L_y = 1\ m$ and the speed of sound $c = 1\ m/s$. The investigated structure is excited from the right end with an impulsive pressure applied at time $t = 0$ while the rest of the boundaries are sound hard boundary ($v = 0\ m/s$). The boundaries are discretized with 24 equal length linear elements and the time step is taken as $\Delta t = 0.6\Delta x/c$. Pressure responses for three points on the midsection line obtained by the full model are shown in Fig. 2 with an analytical solution for the first 12 seconds, however, the final simulation time used in the error calculation is 25 seconds.

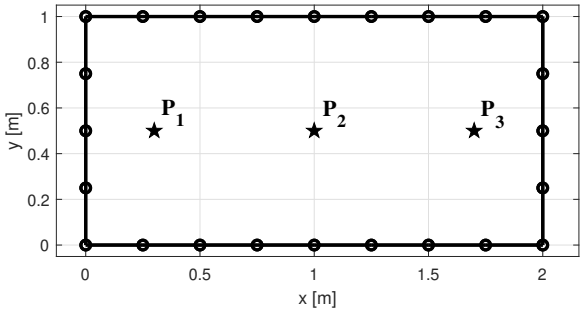

Figure 1. Rectangular interior geometry and three response locations

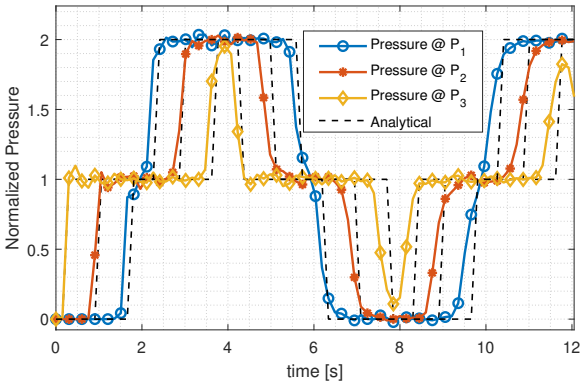

Figure 2. Response obtained from full model at three points to impulsive pressure

Next, the effect of δ is examined by means of the error defined as the L_2 norm of the maximum difference between

full solution and series expanded solution on three points in the domain, shown mathematically as

$$\epsilon = \sqrt{\sum_{i=1}^{3} \left(\max_{t \in T} \left(p_i^{\text{full}}(t) - p_i^{\text{series}}(t) \right) \right)^2}. \qquad (12)$$

Fig. 3 demonstrates the decrease of error for increasing order of expansion while considering $r_{rep} = r_{avg}$. This decrease only continues up to a $\delta = \delta_c$ value after which the error starts to increase with increasing order of the expansion. For the δ values larger than δ_c, the $t > r_{max}/c$ assumption is not satisfied, such that the effect of the Heaviside step function needs to be taken into account. This inclusion changes the kernel that is approximated, which nullifies the earlier series expansion, resulting in a problem dependent causality limit δ_c after which no convergence can be obtained. Note that, calculating δ with $r = r_{max}$ would be a better metric so that $\delta_c \approx 1$ for all problems; however, to stick to the historical convention r_{avg} is used while calculating δ.

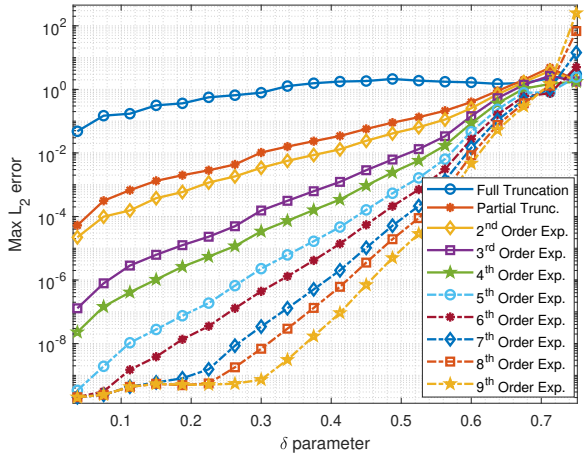

Figure 3. Change of error due to series expansion for different expansion orders for rectangular geometry

By choosing an acceptable error of 10^{-3}, Tab. 1 is constructed indicating the largest reduction achieved within the error limit for certain reduction orders. A clear benefit of using higher orders on the storage and construction costs can be noticed, with diminishing returns. For the sake of completeness, results obtained from [12] are also included in Tab. 1, although no error is specified in the paper.

Table 1. Reduction percentages for given orders of reduction for absolute error of 10^{-3}

Order	None	1st	2nd	3rd	5th	9th	[12]
Reduction	0%	38%	55%	76%	82%	83%	70%

4.2 Exterior response for a circular geometry with time harmonic boundary excitation

The second investigated example is the exterior problem of the circular geometry shown in Fig. 4 with radius of $1\ m$, and with $c = 1\ m/s$. The geometry is excited on all boundaries with time harmonic pressure starting at time $t = 0$ with the frequency of $f = 0.5\ Hz$. The boundary is discretized with 24 equal length linear elements and the time step is taken as $\Delta t = 0.6\Delta x/c$. The time response for three different points inside the domain at different distances away from the center obtained by the full model can be seen in Fig. 5 with analytical results for the first 5 seconds but is used in error analysis with 25 seconds total time.

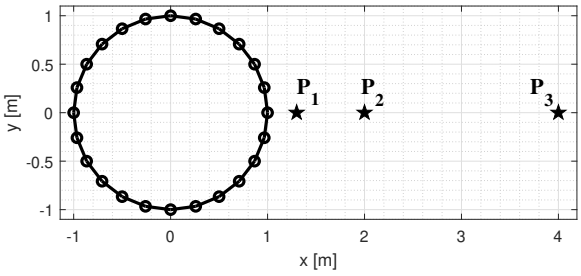

Figure 4. Circular exterior geometry and three response locations

The effect of δ on the error defined by Eqn. (12) is shown in Fig. 6 by considering $r_{rep} = r_{avg}$. The error is greatly reduced compared to full truncation even by including the first order term (partial truncation approach). Similarly to the interior example of Sec. 4.1, in case δ is larger than δ_c, the error starts to increase with increasing order of terms. Note that compared to the interior example, including even orders in the expansion does not offer a significant improvement to the error.
Similarly, choosing an acceptable error as 10^{-3} Tab. 2 can be constructed as is done in Sec. 4.1. Unlike the first example, reduction decreases with second order which is counterintuitive; where an explanation will be given in Sec. 4.4.

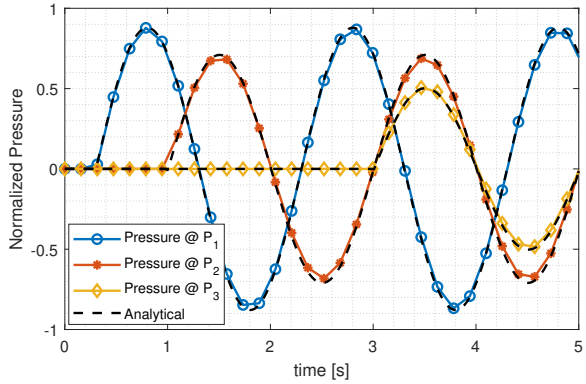

Figure 5. Response obtained from full model at three points to time-harmonic pressure

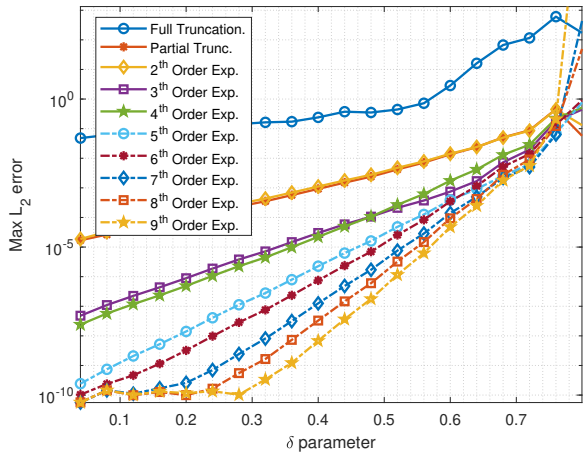

Figure 6. Change of error due to series expansion for different expansion orders for circular geometry

Table 2. Reduction percentages for given orders of reduction for absolute error of 10^{-3}

Order	None	1st	2nd	3rd	5th	9th
Reduction	0%	75%	67%	87%	86%	84%

4.3 Exterior response of a complex geometry with a full sine plane wave excitation

The examined exterior complex geometry is shown in Fig. 7 with $c = 343\ m/s$. The geometry is excited by a propagating single period full sine wave with a frequency of $f = 171.5\ Hz$, which starts propagating at $y = 3\ m$ at time $t = 0$ directed towards negative y-direction. The boundaries are considered sound hard, while they are discretized with $\sim 0.15\ m$ linear elements and the time step is taken as $\Delta t = 0.6\Delta x/c$. The time response for the first 0.04 seconds obtained through the full model is given in Fig. 8.

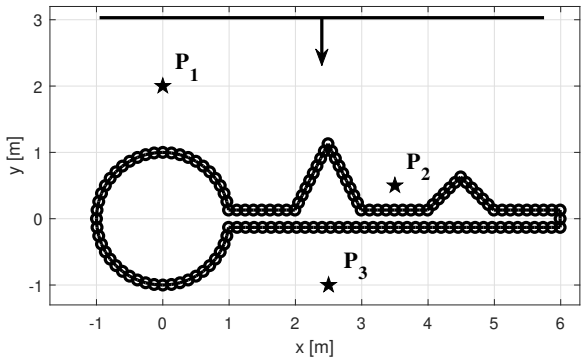

Figure 7. Complex exterior geometry with three response locations

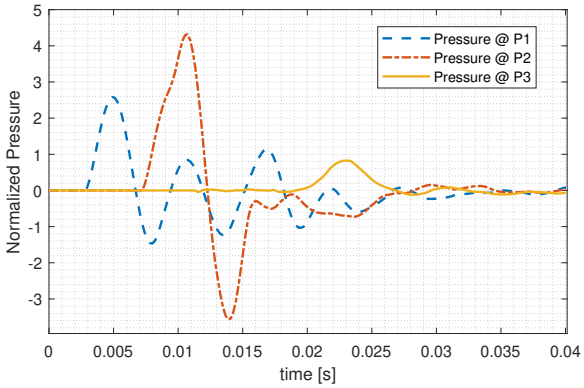

Figure 8. Response obtained from full model at three points to a full sine traveling wave

The effect of δ is examined in Fig. 9 by considering $r_{rep} = r_{avg}$. Unlike the examples of Sec. 4.1 and Sec. 4.2, the reduction that is achieved by increasing the approximation order is lower. Moreover, due to the large size of the geometry compared to the total simulation time, δ_c is much smaller, which limits the reduction as well. Similar error table can be constructed for this example as well, however, the trend is similar to Tab. 1 where the reduction stagnates around 50% starting from second order expansion for 10^{-3} error criteria.

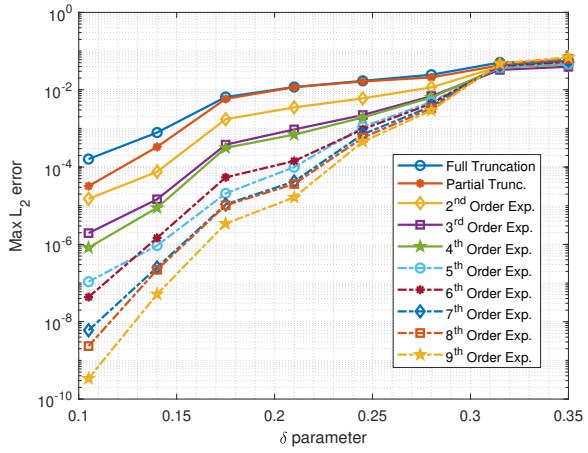

Figure 9. Change of error due to series expansion for different expansion orders for complex geometry

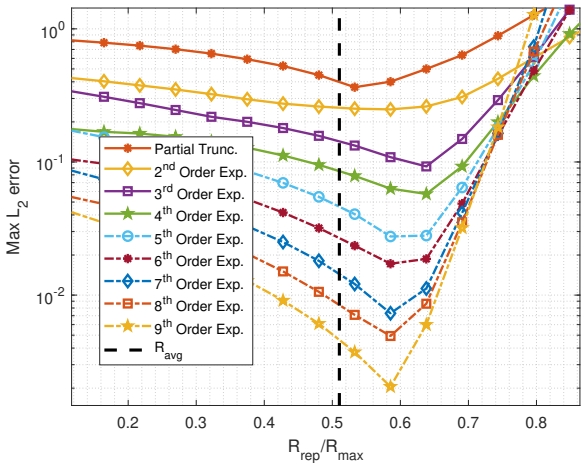

Figure 10. Change of error with changing representative distance for different expansion orders for the problem of Sec. 4.1 using $\delta = 0.6$

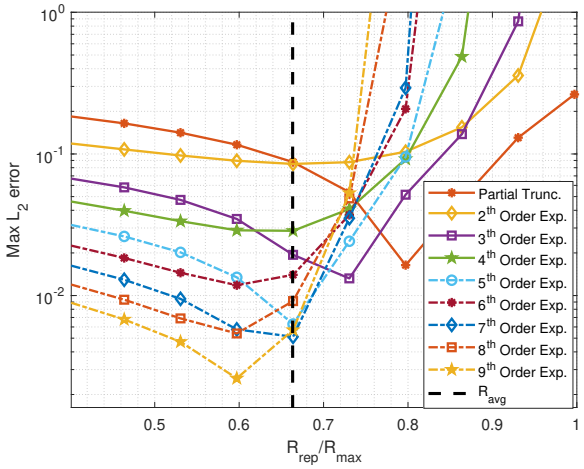

Figure 11. Change of error with changing representative distance for different expansion orders for the problem of Sec. 4.2 using $\delta = 0.7$

4.4 Choice of representative distance

Even though employing $r_{rep} = r_{avg}$ within the Taylor expansion is a logical choice, it might be suboptimal in terms of the induced approximation error. To examine the effect of this selection on the approximation error, consecutive error analyses are performed by keeping δ constant and changing r_{rep} for a given expansion order. Inspecting Fig. 10 given for the problem of the Sec. 4.1 using $\delta = 0.6$, it is clear that the optimum choice for each expansion order changes, converging to a general optimum around $r = 0.6r_{max}$, which is slightly different than r_{rep} used Sec. 4.1. Even though, the difference is small, using the optimal r_{rep} affects the maximum error significantly, which is approximately halved.

Similar conclusions can be drawn for the exterior problem of Sec. 4.2 as given in Fig. 11 for $\delta = 0.7$. An opposite trend compared to interior case is observed with optimal distance decreasing for increasing order, while changes are more chaotic. Moreover, addition of even order terms increases the optimum error significantly.

Based on these conclusions, the need for a good apriori error estimator becomes pronounced, since the error strongly depends on the expansion distance while increasing the expansion order might not reduce the error if the same expansion distance is used.

5. CONCLUSION

In this work, the truncation method for 2D acoustic TD-BEM is extended using a Taylor series expansion. The proposed approach offers considerable savings for both storage and computational costs by increasing the approximation order compared to partial or total truncation method.

One of the main drawbacks of the method is the causality limit δ_c, which depends on the size of the domain. Further reduction after δ_c is not possible and error increases with increasing approximation order. Another drawback of the proposed approach is the lack of an apriori error estimator, which is required for the selection of optimal r_{rep}. Since

the choice of optimal r_{rep} parameter is significantly dependent on the considered geometry, selecting it as r_{avg} can still be a safe option without an apriori error estimator.

Even with aforementioned shortcomings the increase in speed and reduction in memory for interior or exterior problems are quite significant compared to alternative methods. Moreover, reduction in temporal calculations does not hinder any possible spatial size reductions such as model order reduction; which could be combined directly with the temporal reduction introduced in this work.

6. ACKNOWLEDGMENTS

The research of D. Kılıçarslan is funded by "Design for IGA-type discretization workflows (GECKO)" project which receives funding from the European Union's Horizon Europe research and Innovation programme under grant agreement No 101073106 Call: HORIZON-MSCA-2021-DN-01. Views and opinions expressed are however those of the authors only and do not necessarily reflect those of the European Union. The European Union cannot be held responsible for them.

7. REFERENCES

[1] L. Gaul, M. Kögl, and M. Wagner, *Boundary Element Methods for Engineers and Scientists*. Berlin, Heidelberg: Springer Berlin Heidelberg, 2003.

[2] Y. J. Liu, S. Mukherjee, N. Nishimura, M. Schanz, W. Ye, A. Sutradhar, E. Pan, N. A. Dumont, A. Frangi, and A. Saez, "Recent Advances and Emerging Applications of the Boundary Element Method," *Applied Mechanics Reviews*, vol. 64, p. 030802, May 2011.

[3] J. Huijssen, R. Hallez, B. Pluymers, and W. Desmet, "A synthesis procedure for pass-by noise of automotive vehicles employing numerically evaluated source–receiver transfer functions," *Journal of Sound and Vibration*, vol. 332, pp. 3790–3802, July 2013.

[4] J. A. Hargreaves, L. R. Rendell, and Y. W. Lam, "A framework for auralization of boundary element method simulations including source and receiver directivity," *The Journal of the Acoustical Society of America*, vol. 145, pp. 2625–2637, Apr. 2019.

[5] H. Wang, D. Henwood, P. Harris, and R. Chakrabarti, "Concerning the cause of instability in time-stepping boundary element methods applied to the exterior acoustic problem," *Journal of Sound and Vibration*, vol. 305, pp. 289–297, Aug. 2007.

[6] A. Aimi, M. Diligenti, C. Guardasoni, I. Mazzieri, and S. Panizzi, "An energy approach to space–time Galerkin BEM for wave propagation problems," *International Journal for Numerical Methods in Engineering*, vol. 80, pp. 1196–1240, Nov. 2009.

[7] C. Lubich, "Convolution quadrature and discretized operational calculus. II," *Numerische Mathematik*, vol. 52, pp. 413–425, July 1988.

[8] J. Dominguez, *Boundary elements in dynamics*. International series on computational engineering, Southampton Boston London New York: Computational mechanics publ. Elsevier applied science, 1993.

[9] V. Demirel and S. Wang, "An efficient boundary element method for two-dimensional transient wave propagation problems," *Applied Mathematical Modelling*, vol. 11, pp. 411–416, Dec. 1987.

[10] W. J. Mansur and W. Delima-Silva, "Efficient time truncation in two-dimensional bem analysis of transient wave propagation problems," *Earthquake Engineering & Structural Dynamics*, vol. 21, pp. 51–63, Jan. 1992.

[11] D. Soares and W. Mansur, "An efficient time-truncated boundary element formulation applied to the solution of the two-dimensional scalar wave equation," *Engineering Analysis with Boundary Elements*, vol. 33, pp. 43–53, Jan. 2009.

[12] J. Carrer, W. Pereira, and W. Mansur, "Two-dimensional elastodynamics by the time-domain boundary element method: Lagrange interpolation strategy in time integration," *Engineering Analysis with Boundary Elements*, vol. 36, pp. 1164–1172, July 2012.

[13] W. J. Mansur, *A Time-Stepping Technique to Solve Wave Propagation Problems Using The Boundary Element Method*. PhD, University of Southampton, Soputhampton, UK, Sept. 1983.

[14] J. A. M. Carrer and W. J. Mansur, "Time-dependent fundamental solution generated by a not impulsive source in the boundary element method analysis of the 2D scalar wave equation," *Communications in Numerical Methods in Engineering*, vol. 18, pp. 277–285, Apr. 2002.